

3D QSAR studies on T-type calcium channel blockers using CoMFA and CoMSIA

Munikumar Reddy Doddareddy, Hee Kyung Jung, Joo Hwan Cha, Yong Seo Cho,
Hun Yeong Koh, Moon Ho Chang and Ae Nim Pae*

Biochemicals Research Center, Korea Institute of Science and Technology, PO Box 131, Cheongryang, Seoul 130–650, South Korea

Received 6 January 2004; revised 20 January 2004; accepted 21 January 2004

Abstract—Comparative molecular field analysis (CoMFA) and comparative molecular similarity indices analysis (CoMSIA) were performed on a series of isoxazolyl compounds as a potent T-type calcium channel blockers. A set of 24 structurally similar compounds served to establish the model. Four different conformations of the most active compound were used as template structures for the alignment, three of which were obtained from Catalyst pharmacophore modeling and one by using SYBYL random search option. All CoMFA and CoMSIA models gave cross-validated r^2 (q^2) value of more than 0.5 and conventional r^2 value of more than 0.85. The predictive ability of the models was validated by an external test set of 10 compounds, which gave satisfactory pred r^2 values ranging from 0.577 to 0.866 for all models. Best predictions were obtained with CoMFA std model of Conformer no: 3 alignment ($q^2=0.756$, $r^2=0.963$), giving predictive r^2 value of 0.866 for the test set. CoMFA and CoMSIA contour maps were used to analyze the structural features of the ligands accounting for the activity in terms of positively contributing physicochemical properties: steric, electrostatic, hydrophobic and hydrogen bonding fields.

© 2004 Elsevier Ltd. All rights reserved.

1. Introduction

Calcium channel blockers (CCBs) are widely used for the treatment of patients with stable angina pectoris, hypertension and variant angina.^{1–3} CCBs are a heterogeneous group of drugs that inhibit inward calcium channel current to a variable degree in different tissues including the vascular smooth muscle, myocardium, and sinus and atrioventricular (AV) nodes.^{1,2} First generation CCBs (nifedipine, diltiazem, verapamil) all block L-type calcium channels and are classified as dihydropyridine (e.g., nifedipine) or non-DHP agents such as phenylalkylamines (e.g., verapamil) and benzothiazepines (e.g., diltiazem). The second and third generations CCBs are either slow-release or long-acting formulations of the first generation CCBs, examples such as amlodipine or felodipine. But most of the CCBs have been used in the therapy of hypertension and angina pectoris feature to some extent unwanted effects such as negative inotropism, atrioventricular blockade or neurohormonal activation,^{1–3} which often limit their

therapeutic use. In addition to conventional L-type calcium channels, there are T-type calcium channels, which play important role in the initial depolarization of sinus and AV nodes.^{4,5} Blockade of these channels slows the sinus rate and prolongs AV nodal conduction, in addition to causing vasodilation, without adverse negative inotropic or positive chronotropic cardiac actions.^{6,7} Most important example of the selective T-type calcium channel blockers is mibefradil, which was introduced to the market in 1997, then abruptly withdrawn. It was approved for use in hypertension and angina and marketed as the first selective T-type calcium channel blocker.⁸ Indeed, depending on the cell type, mibefradil blocks T-type calcium channels 10–30 times more potently than L-type calcium channels.^{9,10} In addition, mibefradil is highly tissue selective, relaxing smooth muscle without inducing reflex tachycardia, or having much effect on cardiac chronotropy or inotropy.^{8,11} However, pharmacokinetic interactions⁴ with other drugs metabolized by cytochromes P-450 3A4 and 2D6 (e.g., antihistamines such as astemizole) and post-marketing data showing an increase in mortality in the elderly who were also taking β -blockers and DHP-type CCBs and reports of rhabdomyolysis with concomitant simvastatin therapy,^{12,13} eventually led to the with-

* Corresponding author. Tel.: +82-2958-5185; fax: +82-2958-5189;
e-mail: anpae@kist.re.kr

drawal of mibefradil^{14,15} from the clinic. As a part of on going work on T-type calcium channel blockers devoid of adverse effects like that on cytochrome P-450 3A4, we studied quantitative structure–activity relationship of piperazinylalkylisoxazole compounds¹⁶ (Table 1) synthesized in our laboratory to gain insight into steric, electrostatic, hydrophobic and hydrogen bonding properties influencing the activity.

In this paper, two 3D QSAR methods, CoMFA and CoMSIA, were applied to investigate the local physico-chemical properties involved in the interaction between ligand and receptor. The widely used CoMFA (comparative molecular field analysis) calculates steric and electrostatic properties according to Lennard-Jones and Coulomb potentials.¹⁶ Similar to the usual CoMFA approach, CoMSIA data table^{18–20} (comparative molecular similarity indices analysis) is constructed from similarity indices calculated via common probe atom which is placed at the intersections of regularly spaced lattice. CoMSIA is believed to be less affected by interpretable contour maps as result of employing Gaussian type distance dependence with the molecular similarity

indices it uses.¹⁸ Further more, in addition to steric and electrostatic fields of CoMFA, CoMSIA defines explicit hydrophobic and hydrogen bond donor and acceptor descriptor fields.

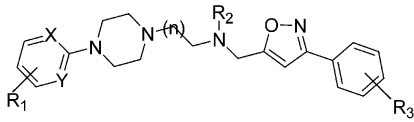
The contour maps derived from both the CoMFA and CoMSIA models permitted an understanding of the steric, electrostatic, lipophilic and hydrogen bonding requirements for ligand binding. As a consequence, the structural variations in the training set that give rise to variations in the molecular fields at particular regions of the space are correlated to biological activities serving as a guide to the design of novel inhibitors.

2. Materials and methods

2.1. Dataset

The training set comprises of a series of 24 highly flexible piperazinylalkylisoxazole compounds with IC₅₀ values ranging from 1.02 to 60.54 μmol. The biological activities (IC₅₀ data) on HEK 293 cell with stabilized

Table 1. Structures and biological activities of molecules used in training and test sets



Compd	R ₁	R ₂	R ₃	n	X	Y	IC ₅₀
Training set							
1	3-Trifluoromethyl	H	[1,3] Dioxolane	1	C	C	2.98
2	3-Trifluoromethyl	H	2-Trifluoromethyl	1	C	C	1.02
3	3-Trifluoromethyl	H	2,3-Dimethoxy	1	C	C	3.33
4	3-Trifluoromethyl	H	2-Nitro	1	C	C	3.06
5	4-Flouro	H	2-Methoxy	1	C	C	10.41
6	4-Flouro	H	2-Nitro	1	C	C	9.26
7	H	H	2-Methoxy	1	C	C	19.13
8	H	H	2-Trifluoromethyl	1	C	C	5.82
8	4-Methyl	H	[1,3] Dioxolane	1	C	C	7.62
10	4-Methyl	H	2-Methoxy	1	C	C	8.19
11	4-Methyl	H	2-Trifluoromethyl	1	C	C	2.51
12	4-Methyl	H	2,3-Dimethoxy	1	C	C	4.06
13	4-Methyl	H	2-Flouro	1	C	C	7.55
14	4-Methyl	H	2,3-Phenyl	1	C	C	8.46
15	4-Methyl	H	2-Nitro	1	C	C	4.83
16	4-Methyl	H	[1,4] Dioxane	1	C	C	7.49
17	H	H	2-Methoxy	1	C	N	60.54
18	H	H	2-Trifluoromethyl	1	C	N	8.82
19	4-Methyl	H	2-Trifluoromethyl	2	C	C	4.75
20	H	Methyl	[1,3] Dioxolane	1	C	C	5.49
21	H	Methyl	2-Methoxy	1	C	C	10.71
22	H	Methyl	2-Trifluoromethyl	1	C	C	4.21
23	H	Ethyl	2-Methoxy	1	C	N	18
24	H	Ethyl	2-Trifluoromethyl	1	C	N	7.01
Test set							
25	3-Chloro	H	2-Methoxy	1	C	C	7.49
26	H	H	2-Methoxy	1	N	N	53.2
27	H	H	2-Trifluoromethyl	1	N	N	8.24
28	3-Trifluoromethyl	H	2-Methoxy	1	C	C	2.04
29	2,4-Dimethyl	H	2-Trifluoromethyl	1	C	C	1.53
30	4-Flouro	H	2-Trifluoromethyl	1	C	C	2.54
31	3-Trifluoromethyl	H	2-Trifluoromethyl	2	C	C	2.71
32	2,4-Dimethyl	H	2-Trifluoromethyl	2	C	C	4.17
33	4-Flouro	Methyl	2-Methoxy	1	C	C	4.36
34	H	Methyl	2-Trifluoromethyl	1	C	N	10.56

IC₅₀ values were measured by HEK 293 cell assay.

α 1G T-type calcium channel for the training set were converted to pIC_{50} ($-\log IC_{50}$) values and used as dependent variables in the CoMFA and CoMSIA analyses. The predictiveness of each derived model was evaluated using an external test set of 10 compounds (Table 1) with IC_{50} values ranging from 1.53 to 53.2 μ mol which are within the activity range of training set.

2.2. Molecular modeling and alignment

All Molecular modeling calculations were performed using SYBYL program,²¹ package version 6.9 on silicon graphics origin 300 with IRIX 6.5 operating system. Energy minimizations were performed using Tripos force field²¹ and Gasteiger Huckel charge with distance dependent dielectric and conjugate gradient method with convergence criterion of 0.01 kcal/mol. The most important requirement for CoMFA and CoMSIA studies is that the 3D structures to be analyzed are aligned according to a suitable conformational template, which is assumed to be a 'bioactive' conformation.¹⁷

As no structural information is available about ligand–receptor complexes, we used three conformations of most active compound mapping to three different pharmacophores developed by using Catalyst²³ pharmacophore modeling²⁴ and one low energy conformation by using SYBYL random search option as templates for the alignment (Fig. 1). We felt this as most appropriate because not always the minimum energy conformation is the bioactive conformation. Further more as all the molecules of the training set are highly flexible with each containing 7 to 8 rotatable bonds, we used an innovative method of automatic alignment wherein all mole-

cules were sketched from 'conformer' of the most active compound **2** and subsequent minimization was done by using maximum 30 iterations so that there is no appreciable change in conformation. The energies of all molecules of the training set and test set aligned to 4 different conformational templates were given in Table 2. As expected low energy conformations for all compounds were obtained in random search conformer alignment (Conf No: 3).

2.3. CoMFA and CoMSIA 3D QSAR models

The steric and electrostatic potential fields for CoMFA were calculated at each lattice intersection of a regularly spaced grid of 2.0 Å. The lattice was defined automatically, and is extended 4 Å units past Vanderwaals volume of all molecules in X, Y, and Z directions. The Vanderwaals potential (Lennard-Jones 6–12) and columbic term, which represent steric and electrostatic fields respectively, were calculated using Tripos force field.²² A distance dependent dielectric expression $\epsilon = \epsilon_0.R_{ij}$ with $\epsilon = 1.0$ was used. An sp^3 carbon atom with vanderwaals radius of 1.52 Å and +1.0 charge was served as the probe atom to calculate steric and electrostatic fields. The steric and electrostatic contributions were truncated to ± 30 kcal/mol, and electrostatic contributions were ignored at lattice intersections with maximum steric interactions. The CoMFA steric and electrostatic fields generated were scaled by CoMFA standard option given in SYBYL.

CoMSIA similarity indices descriptors were derived according to Klebe et al¹⁷ with same lattice box as was used for the CoMFA calculations, with a grid spacing

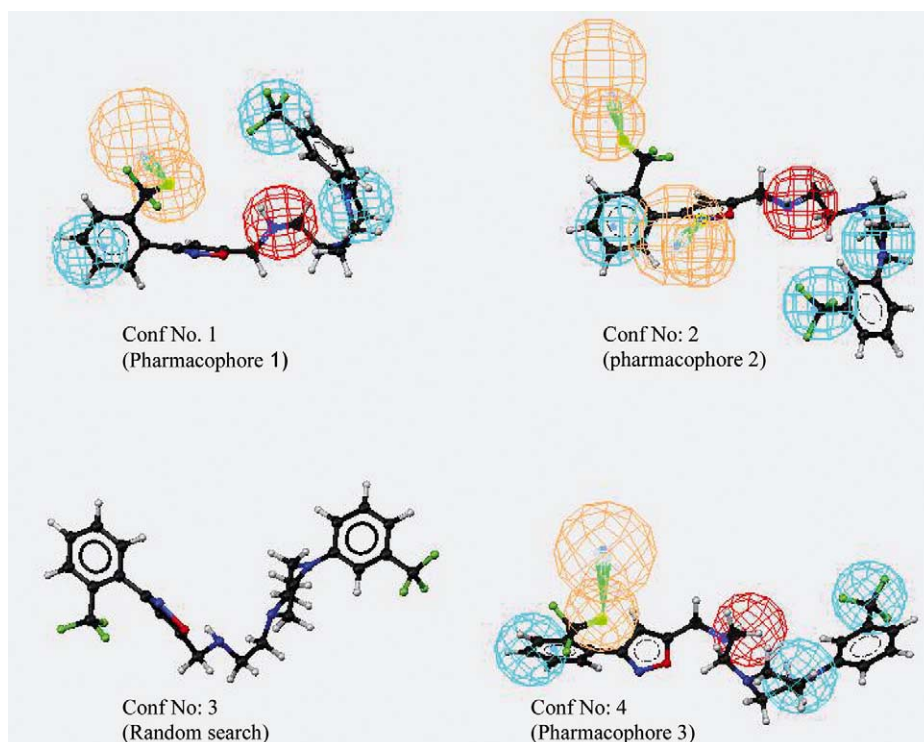


Figure 1. Four different conformations of the most active compound **2** used for alignment. (3rd conformer is obtained from random search).

Table 2. Conformational energies of all molecules used in analyses

Compd	Conf No1	Conf No2	Conf No3	Conf No4
Training set				
1	47.56	56.42	43.69	47.87
2	32.58	38.36	23.91	27.21
3	45.84	53.24	32.62	35.83
4	37.79	42.45	31.02	34.57
5	28.91	39.04	24.88	28.66
6	35.73	41.53	29.15	32.73
7	29.53	39.99	26.01	29.77
8	29.8	37.74	23.33	26.88
9	48.73	54.62	42.26	46.5
10	28.68	39.38	25.39	29.14
11	28.65	37.14	22.7	26.26
12	49.17	51.36	31.28	34.44
13	32.68	38.02	24.75	28.52
14	37.12	41.7	29.29	33.43
15	34.23	41.99	29.66	33.22
16	39.35	45.61	32.94	36.88
17	36.27	35.88	24.24	27.07
18	27.44	35.55	21.5	24.51
19	32.31	48.67	34.85	29.32
20	48.72	56.88	44.83	46.66
21	29.69	42.19	27.65	29.29
22	29.37	39.62	25.47	26.36
23	35.01	39.72	27.47	26.76
24	26.91	37.84	25.58	23.91
Test set				
25	30.76	38.11	25.95	28.86
26	26.72	32.57	20.66	23.56
27	26.28	30.41	17.3	20.8
28	42.19	40.55	26.9	30.17
29	33.24	43.58	23.27	27.42
30	29.63	36.65	22.21	25.76
31	35.17	46.04	32.57	30.2
32	35.71	46.79	34.65	36.21
33	28.92	41.21	26.64	28.18
34	27.03	35.81	23.69	23.95

In kcal/mol, electrostatics also included.

of 2 Å employing a C⁺ probe atom with a radius of 1.0 Å as implemented in SYBYL. CoMSIA similarity indices (A_F) for a molecule j with atoms i at a grid point q are calculated by eq 1 as follows.

$$A_{F,k}^q(j) = - \sum \omega_{\text{probe},k} \omega_{ik} e^{-\alpha r} \quad (1)$$

Five physicochemical properties k (steric, electrostatic, hydrophobic, hydrogen bond donor, and hydrogen bond acceptor) were evaluated using the probe atom. A Gaussian type distance dependence was used between the grid point q and each atom i of the molecule. The default value of 0.3 was used as the attenuation factor (α). In CoMSIA, the steric indices are related to the third power of the atomic radii, the electrostatic descriptors are derived from atomic partial charges, the hydrophobic fields are derived from atom-based parameters developed by Viswanadhan et al.,²⁵ and the hydrogen bond donor and acceptor indices are obtained by a rule-based method derived from experimental values.²⁶

2.4. PLS calculations and validations

Partial least-square (PLS)^{27, 28} methodology was used for all 3D QSAR analyses. Column filtering was set to

1.0 kcal/mol to speed up the analysis and reduce the noise. The CoMFA and CoMSIA descriptors were used as independent variables, and pIC₅₀ values were used as dependent variables in partial least-squares regression analyses to derive 3D QSAR models using the standard implementation in the SYBYL package. The predictive value of the models was evaluated first by leave-one-out (LOO)^{29,30} cross-validation. The cross-validated coefficient, q^2 , was calculated using eq 2

$$q^2 = 1 - \frac{\sum (Y_{\text{predicted}} - Y_{\text{observed}})^2}{\sum (Y_{\text{observed}} - Y_{\text{mean}})^2} \quad (2)$$

Where $Y_{\text{predicted}}$, Y_{observed} and Y_{mean} are predicted, actual, and mean values of the target property (pIC₅₀), respectively. $\sum (Y_{\text{predicted}} - Y_{\text{observed}})^2$ is the predictive sum of squares (PRESS). To maintain the optimum number of PLS components and minimize the tendency to over fit the data, the number of components corresponding to the lowest PRESS value was used for deriving the final PLS regression models. In addition to the q^2 and number of components, the conventional correlation coefficient r^2 and its standard error s (SEE) were also computed. To further assess the robustness and statistical confidence of the derived models, bootstrapping analysis²⁸ (10 runs) were performed and the mean r^2 is given as q^2 bootstrap. A total of 24 CoMFA and CoMSIA models were derived from 4 different alignments whose statistical data is given in Tables 3–6. All models gave satisfactory LOO crossvalidated q^2 value of more than 0.5 and except CoMFA (std+Hbond) model of Conf No: 2 alignment (which is a 2 component model) all of them gave conventional r^2 value of more than 0.85 indicating their predictive ability.

2.5. Predictive r squared (r^2 pred)

To validate the derived CoMFA and CoMSIA models, biological activities of an external test set of 10 compounds (Table 1) were predicted using models derived from the training set. The predictive ability of the models is expressed by predictive r^2 value, which is analogous to crossvalidated r^2 (q^2) and is calculated by using the formula

$$r_{\text{pred}}^2 = \frac{\text{SD-PRESS}}{\text{SD}} \quad (3)$$

Where SD is the sum of squared deviation between the biological activities of the test set molecule and the mean activity of the training set molecules and PRESS is the sum of squared deviations between the observed and the predicted activities of the test molecules. Except CoMFA (std+Hbond) model of Conf No: 2 alignment (which is a 2 component model) all the other models, gave satisfactory r_{pred}^2 values (Table 7) ranging from 0.577 to 0.866. Best predictions were obtained with CoMFA std model of 'Conf No: 3' alignment ($q^2=0.756$, $r^2=0.963$), giving predictive r^2 value of 0.866 for the test set.

Table 3. Summary of PLS analyses (Conformer No: 1 alignment)

	q ²	N	r ²	SEE	F	SEP	q ² bs	SD
CoMFA std	0.643	4	0.932	0.1	64.609	0.228	0.964	0.023
CoMFA std + Hbond	0.704	7	0.986	0.049	166.66	0.226	0.988	0.006
CoMSIA Steric + electrostatic	0.667	3	0.893	0.122	55.612	0.214	0.903	0.047
CoMSIA Steric + electro + Hydrophobic	0.655	5	0.912	0.116	37.16	0.23	0.951	0.016
CoMSIA Steric + electro + acceptor	0.673	5	0.902	0.123	33.028	0.224	0.933	0.042
CoMSIA All 5 Descriptors	0.65	5	0.869	0.142	23.967	0.232	0.909	0.03

q²—LOO cross validated correlation coefficient, N—optimum number of components, r²—non cross validated correlation coefficient, SEE—standard error of estimate, F—F-test value, SEP—standard error of prediction, q²bs—mean r² of boot strapping analysis (10 runs), SD—standard deviation.

Table 4. Summary of PLS analyses (Conformer No: 2 alignment)

	q ²	N	r ²	SEE	F	SEP	q ² bs	SD
CoMFA std	0.745	5	0.945	0.092	61.69	0.198	0.972	0.01
CoMFA std + Hbond	0.548	2	0.781	0.17	37.508	0.244	0.753	0.079
CoMSIA Steric + electrostatic	0.754	6	0.946	0.094	49.52	0.2	0.978	0.011
CoMSIA Steric + electro + Hydrophobic	0.763	4	0.924	0.105	57.523	0.186	0.933	0.035
CoMSIA Steric + electro + acceptor	0.714	6	0.925	0.11	35.046	0.216	0.955	0.017
CoMSIA All 5 Descriptors	0.702	6	0.907	0.123	27.6	0.22	0.948	0.026

q²—LOO cross validated correlation coefficient, N—optimum number of components, r²—non cross validated correlation coefficient, SEE—standard error of estimate, F—F-test value, SEP—standard error of prediction, q²bs—mean r² of boot strapping analysis (10 runs), SD—standard deviation.

Table 5. Summary of PLS analyses (Conformer No: 3 alignment)

	q ²	N	r ²	SEE	F	SEP	q ² bs	SD
CoMFA std	0.756	6	0.963	0.077	73.89	0.199	0.975	0.01
CoMFA std + Hbond	0.699	8	0.985	0.053	119.173	0.236	0.991	0.006
CoMSIA Steric + electrostatic	0.666	6	0.934	0.104	40.145	0.233	0.966	0.016
CoMSIA Steric + electro + Hydrophobic	0.651	6	0.936	0.102	41.566	0.238	0.959	0.023
CoMSIA Steric + electro + acceptor	0.687	4	0.88	0.132	34.85	0.213	0.912	0.033
CoMSIA All 5 Descriptors	0.688	6	0.895	0.131	24.162	0.225	0.947	0.023

q²—LOO cross validated correlation coefficient, N—optimum number of components, r²—non cross validated correlation coefficient, SEE—standard error of estimate, F—F-test value, SEP—standard error of prediction, q²bs—mean r² of boot strapping analysis (10 runs), SD—standard deviation.

Table 6. Summary of PLS analyses (Conformer No: 4 alignment)

	q ²	N	r ²	SEE	F	SEP	q ² bs	SD
CoMFA std	0.752	6	0.986	0.049	192.82	0.201	0.983	0.011
CoMFA std + Hbond	0.647	7	0.986	0.049	160.078	0.247	0.995	0.004
CoMSIA Steric + electrostatic	0.681	9	0.983	0.059	88.121	0.251	0.996	0.003
CoMSIA Steric + electro + Hydrophobic	0.715	6	0.945	0.095	48.491	0.215	0.973	0.015
CoMSIA Steric + electro + acceptor	0.716	5	0.921	0.11	41.972	0.209	0.955	0.027
CoMSIA All 5 Descriptors	0.775	6	0.95	0.09	53.55	0.191	0.966	0.021

q²—LOO cross validated correlation coefficient, N—optimum number of components, r²—non cross validated correlation coefficient, SEE—standard error of estimate, F—F-test value, SEP—standard error of prediction, q²bs—mean r² of boot strapping analysis (10 runs), SD—standard deviation.

Table 7. Predictive r² values of test set of all 24 models

Model	Pred r ²			
	Conf No: 1	Conf No: 2	Conf No: 3	Conf No:4
CoMFA std	0.616	0.78	0.866	0.71
CoMFA std + Hbond	0.68	0.46	0.72	0.583
CoMSIA Steric + electrostatic	0.577	0.823	0.795	0.783
CoMSIA Steric + electro + Hydrophobic	0.712	0.766	0.732	0.713
CoMSIA Steric + electro + acceptor	0.639	0.734	0.646	0.581
CoMSIA All 5 Descriptors	0.698	0.728	0.614	0.708

2.6. QSAR coefficient contour maps

The visualization of the results of all the CoMFA and CoMSIA models have been performed using the 'stDev*Coeff' mapping option contoured by actual values. Counter maps of the models derived from 'Conf No: 3' alignment (Random search) which showed best predictive ability, were used for discussion.

2.7. Results and discussions

CoMFA and CoMSIA 3D QSAR models were derived for a set of 24 structurally similar piperazinyllalkylisoxazole compounds acting as T-type calcium channel blocking agents by using four different conformational alignments (Fig. 1). Total 24 models, six per each alignment were generated (Table 3–6). All models were validated by an external test set of 10 compounds. CoMFA std model ($q^2=0.756$, $r^2=0.963$) of 'Conf No: 3' alignment gave best predictive r^2 value of 0.866 for the test set. The satisfactory statistical data for all the models aligned by using different conformational templates shows that the relative positioning of the biologically important groups that is important than the conformation itself, for getting models with good predictability. The contour plots obtained from the models are representations of the lattice points, where difference in field values is strongly associated with the activity. The use of putative bioactive conformation in the alignment helps us in getting useful interpretations about the active site. In our study even though all 4 conformational alignments gave models with good predictability, any interpretations about ligand–receptor interactions by super imposing contour maps of any particular alignment on active site of a receptor model may give misleading conclusions, as we don't know which one of these 4 conformations is most probably the bioactive one and also from the fact that not always minimum energy conformation is the bioactive conformation. The results of the present study clearly shows that CoMFA and CoMSIA 3D QSAR studies are just a part of ligand based drug design where we can estimate activities of untested compounds by using the information available from already tested compounds and so it has nothing to do with the receptor, unless bioactive conformation is used for alignment, where the

complimentary idea of the contour maps may give information about active site.

The contour maps of CoMFAsd and CoMSIA combined (all descriptors) models of 'conf No: 3' alignment were used to understand the steric, electrostatic, hydrophobic and hydrogen bonding field requirements for ligand binding. Table 5 shows PLS statistics of all the CoMFA and CoMSIA combined models of 'Conf No: 3' alignment.

Figure 2 depicts steric contour maps of CoMFA std and CoMSIA (all descriptors) of 'Conf No: 3' alignment. Sterically favored green regions are found near 3,4-positions of R_1 , all active compounds have either 3-trifluoromethyl or 4-methyl groups to satisfy this. On R_3 side, the 2-position substituents fall in sterically favored regions, where as groups more bulky than methoxy or trifluoromethyl groups will fall in sterically unfavored yellow region and may decrease activity. In addition to these, both models (Fig. 2) showed an extra sterically favored green region occupying methyl and ethyl substituents (R_2) on N, which can be explained from the fact that compounds **21**, **22**, **23** and **24** showed more activity than their respective unsubstituted analogues **7**, **8**, **17** and **18**.

Figure 3 shows electrostatic contour maps of CoMFA std and CoMSIA (all descriptors) of 'Conf No: 3' alignment. Negative charge favored red regions were found near 3-position of R_1 and 2-position of R_3 , where the active compounds contain electronegative atoms like O, N, F in the form of methoxy, nitro and trifluoromethyl groups respectively. On R_1 side, positive charge favored or negative charge unfavored blue region is found on ring, where less active compounds like **18** have electron rich N in the form of pyridine ring.

Figure 4 shows hydrophobic contour maps of CoMSIA (all descriptors) of 'Conf No: 3' alignment. Hydrophobic favored yellow regions were observed around 3-position of R_1 and 2-position of R_3 , where active compounds contain trifluoromethyl groups as substituents. All the four ring systems are invariant in the training set and so they are not accounted for the hydrophobicity in

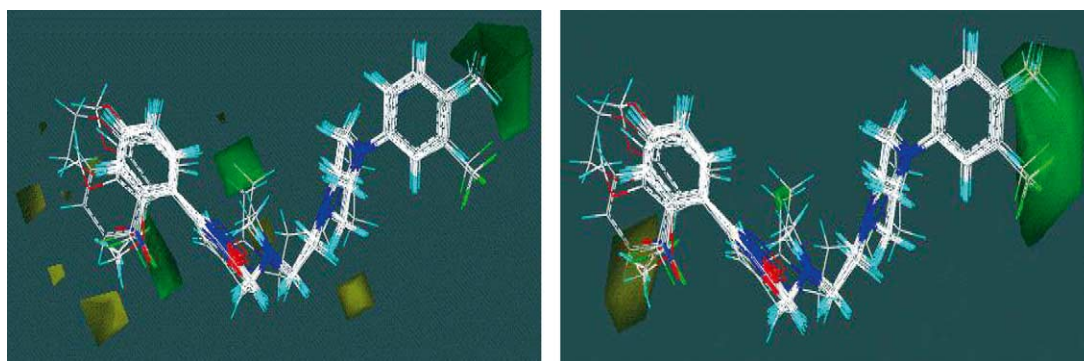


Figure 2. (a) CoMFA std; (b) CoMSIA (all descriptors) stdev*coeff. steric contour plots; green contours indicate regions where bulky groups increase activity, whereas yellow contours indicate regions where bulky groups decrease activity.

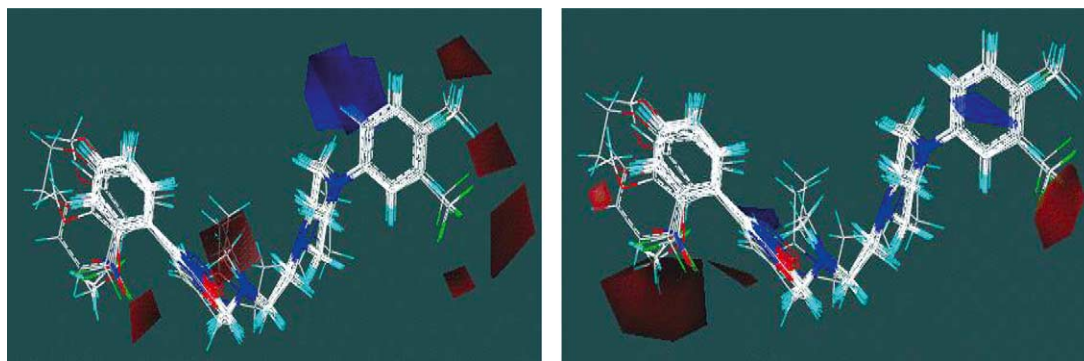


Figure 3. (a) CoMFA std; (b) CoMSIA (all descriptors) stdev*coeff electrostatic contour plots; blue contour indicate regions where positive groups increase activity, whereas red contours indicate regions where negative charge increases activity.

correlation with activity. Hydrophobic unfavored white regions are found at 3-position of the R_3 indicating the importance of polar O either in the form of methoxy group or fused dioxole or dioxane ring systems at these positions for activity.

Figure 5 shows hydrogen bond acceptor contour maps of CoMSIA (all descriptors) of 'Conf No: 3' alignment. Hydrogen bond acceptor field favored magenta region is found at the 2-position of R_3 , where almost all compounds contain acceptor groups in the form of methoxy, nitro, trifluoromethyl groups. We believe this as one of the most important requirements of this series of

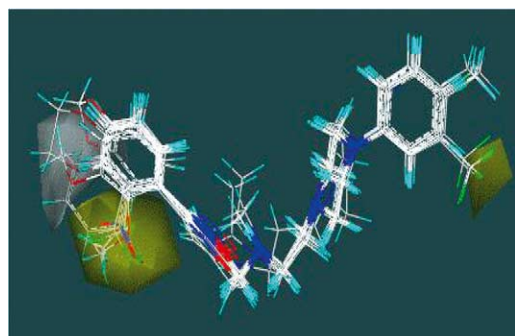


Figure 4. CoMSIA (all descriptors) stdev*coeff hydrophobic contour plots; yellow contours indicate regions where hydrophobic groups increases activity, whereas white contours indicates regions where hydrophobic group decreases activity.

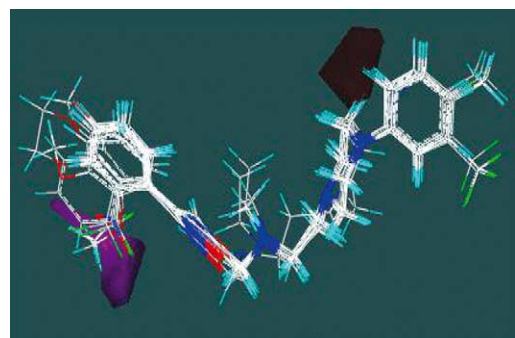


Figure 5. CoMSIA (all descriptors) stdev*coeff. H-bond acceptor plots; magenta contours indicate regions where H-bond acceptor group increases activity, whereas red contours indicate regions where H-bond acceptor group decreases activity.

compounds to show T-type calcium channel blocking activity. The presence of acceptor unfavored red region near nitrogen of the pyridine containing compounds (**17**, **18**, **23** and **24**) indicates the negative effect it shows on their activity.

Figure 6 shows hydrogen bond donor contour maps of CoMSIA (all descriptors) of 'Conf No: 3' alignment. Hydrogen bond donor favored cyan and unfavored violet regions are found at the same position (R_2) surrounding N of amino group giving no clear cut idea about the importance of hydrogen bond donor at this position for activity. This can be explained from the fact that although most of the active compounds contain H donor at this position, compounds **21**, **22**, **23** and **24** which don't have H donor at that position showed more activity than their analogues **7**, **8**, **17** and **18** containing H donor. Interestingly the more activity of the **21**, **22**, **23**, and **24** than their analogues is explained by steric favored green region mapping methyl and ethyl groups at R_2 (Fig. 2).

Comparatively CoMSIA maps are smoother and closer to the involved atoms or functionalities than the corresponding regions in the CoMFA maps making it easier to interpret. It can be observed that, same groups are involved in both steric and hydrophobic favored regions, and also in case of electrostatics and hydrogen bond acceptor fields, where negative charge favored and acceptor favored regions are coinciding and positive

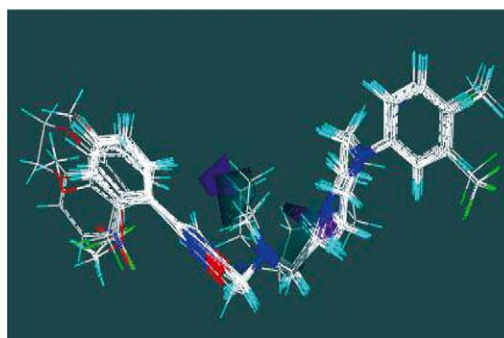


Figure 6. CoMSIA (all descriptors) stdev*coeff. H-bond donor plots; cyan contours indicate regions where H-bond donor group increases activity, whereas purple contours indicate regions where H-bond donor group decreases activity.

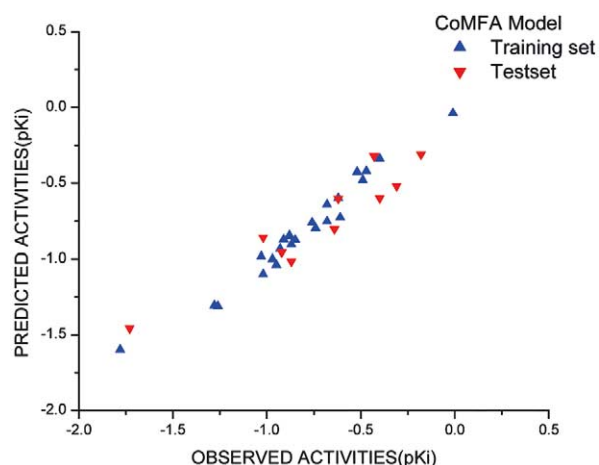


Figure 7. Plot of predicted vs observed values of CoMFA std model, blue triangles show predictions of training set and red triangles show predictions of test set.

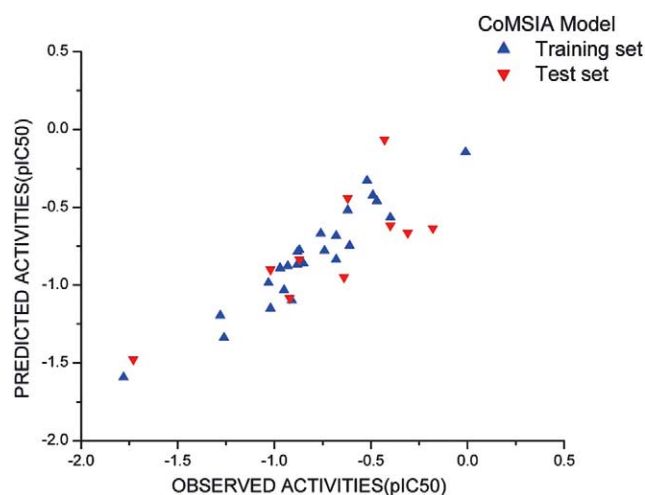


Figure 8. Plot of predicted vs observed values of CoMSIA (all descriptors) model, blue triangles show predictions of training set and red triangles show predictions of test set.

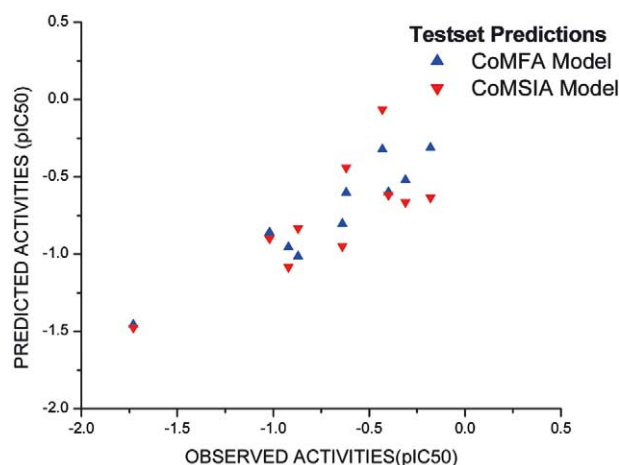


Figure 9. Comparative plot of predicted vs observed values of the test set by both CoMFA std and CoMSIA (all descriptors). CoMFA predictions are shown in blue triangles and CoMSIA predictions are shown in red.

charge favored and acceptor unfavored are near N of pyridine ring containing molecules. The role of isoxazole and piperazine rings is unexplained by these models, as they are 'invariant' in the training set.

Figures 7 and 8 shows plots of observed vs predicted activities of training and test sets of both CoMFA std and CoMSIA (all descriptors) of 'Conf No: 3' alignment respectively. Blue triangles show the predictions of the training set and red shows that of test set. The predictive r^2 values of the test set of both models are 0.866 and 0.614 respectively. Figure 9 shows the comparative plot of predictions of test set by both models. Predictions by CoMFA model are shown in blue triangles and that of CoMSIA models are shown in red.

3. Conclusions

Predictive CoMFA and CoMSIA models were developed for a series of isoxazole compounds as a potent T-type calcium channel blockers by using four different conformations, three of which were obtained from Catalyst pharmacophore modeling and one from random search option, as putative bioactive templates for alignment. All the models were validated by using an external test set of 10 compounds, Best predictions were obtained with CoMFA std model of 'Conf No: 3' alignment ($q^2=0.756$, $r^2=0.963$), giving predictive r^2 value of 0.866 for the test set. CoMFA and CoMSIA 3D-maps obtained from the analyses can be used for the design of new inhibitors in an interactive fashion. The satisfactory statistical data for all the models obtained from different conformational alignments shows that the predictions obtained by superimposing contour maps on active site of a receptor model may be misleading.

Acknowledgements

This work was supported by the Korea Ministry of Science and Technology.

References and notes

- Opie, L. H.; Frishman, W. H.; Thadani, U. Calcium channel antagonists (calcium entry blockers). In: Opie L. H., (Ed.) *Drugs for the Heart*. 4th ed. Philadelphia: WB Saunders; 1999, 50–82.
- Abernethy, D. R.; Schwartz, J. B. *N. Engl. J. Med.* **1999**, *341*, 1447.
- Thadani, U. *Curr. Opin. Cardiol.* **1999**, *14*, 349.
- Asirvatham, S.; Sebastian, C.; Thadani, U. *Drug Safety* **1998**, *19*, 23.
- Triggle, D. J. *J. Hypertens.* **1997**, *15* (5 Suppl), 9.
- Portegies, M. C.; Schmitt, R.; Kraaij, C. J.; Braat, S. H. J. G.; Gassner, A.; Hagemeyer, F.; Ponzenel, H.; Prager, G.; Viersma, J. W.; VanderWall, E. E.; Kleinbloesem, C. H.; Lie, K. I. *J. Cardiovasc. Pharmacol.* **1991**, *18*, 746.
- Cremers, B.; Flesch, M.; Sudkamp, M.; Bohm, M. *J. Cardiovasc. Pharmacol.* **1997**, *29*, 692.

8. Ertel, S. I.; Ertel, E. A.; Clozel, J. P. *Cardiovasc. Drugs Ther.* **1997**, *11*, 723.
9. Mishra, S. K.; Hermsmeyer, K. *Circ. Res.* **1994**, *75*, 144.
10. Benardeau, A.; Ertel, E. Selective block of myocardial T-type calcium channels by mibefradil: A comparison with the 1,4-dihydropyridine, amlodipine, Edited by Clozel, J. P., Nargeot, J., Tsien, R. W., 1997, p 386, Adis international chester, UK.
11. Kobrin, I.; Bieska, G.; Charlon, V.; Lindberg, E.; Pordy, R. *Cardiology* **1998**, *89*, 23.
12. Schmassmann-Suhijar, D.; Bullingham, R.; Gasser, R.; Schmutz, J.; Haefeli, W. E. *Lancet* **1998**, *351*, 1929.
13. Mullins, M. E.; Horowitz, B. Z.; Linden, D. H.; Smith, G. W.; Norton, R. L.; Stump, J. *JAMA* **1998**, *280*, 157.
14. SoRelle, R. *Circulation* **1998**, *98*, 831.
15. Reimer, K. A., Califf, R. M. *Circulation* **1999**, *99*, 198
16. *Bioorg. Med. Chem. Lett.*, submitted for publication.
17. Crammer, R. D., III; Patterson, D. E.; Bunce, J. D. *J. Am. Chem. Soc.* **1988**, *110*, 5959.
18. Klebe, G.; Abraham, U.; Mietzner, T. *J. Med. Chem.* **1994**, *37*, 4130–4139.
19. Klebe, G.; Abraham, U. *J. Comput.-Aided Mol. Design* **1999**, *13*, 1.
20. Bohm, M.; Sturzebecher, J.; Klebe, G. *J. Med. Chem.* **1999**, *42*, 458.
21. SYBYL 6.9. Tripos Inc., 1699 Hanley Road, St. Louis, MO 63144.
22. Clark, M.; Cramer, R. D., III; Van Opdenbosch, N. *J. Comput. Chem.* **1989**, *10*, 982.
23. CATALYST version 4.8 software; ACCELRYN Inc:2001.
24. *Bioorg. Med. Chem.*, accepted for publication.
25. Viswanadhan, V. N.; Ghose, A. K.; Revenkar, G. R.; Robins, R. *J. Chem. Inf. Comput. Sci.* **1989**, *29*, 163.
26. Klebe, G. *J. Mol. Biol.* **1994**, *237*, 212.
27. Wold, S.; Albano, C.; Dunn, W. J.; Edlund, U.; Esbenson, K.; Geladi, P.; Hellberg, S.; Lindberg, W.; Sjostrom, M. In *Chemometrics*; Kowalski, B., Int. Ed.; Reidel: Dordrecht, The Netherlands, 1984, 17.
28. Geladi, P. *J. Chemom.* **1998**, *2*, 231.
29. Cramer, R. D., III; Bunce, J. D.; Patterson, D. E. *Quant. Struct. Act. Relat.* **1988**, *7*, 18.
30. Wold, S. *Technometrics* **1978**, *4*, 397.